

## **AM251 induces apoptosis and G2/M cell cycle arrest in A375 human melanoma cells**

**Running head:** Anti-melanoma activity of AM251

Sara Carpi<sup>a</sup>, Stefano Fogli<sup>a</sup>, Antonella Romanini<sup>b</sup>, Mario Pellegrino<sup>c</sup>, Barbara Adinolfi<sup>a</sup>, Adriano Podestà<sup>d</sup>, Barbara Costa<sup>a</sup>, Eleonora Da Pozzo<sup>a</sup>, Claudia Martini<sup>a</sup>, Maria Cristina Breschi<sup>a</sup>, Paola Nieri<sup>a</sup>

<sup>a</sup>Department of Pharmacy, University of Pisa, Pisa, Italy; <sup>b</sup>University Hospital of Pisa, Pisa, Italy;

<sup>c</sup>Department of Translational Research and New Technologies in Medicine and Surgery, University of Pisa, Pisa, Italy; <sup>d</sup>Department of Veterinary Sciences, University of Pisa, Pisa, Italy

### **Conflicts of interest**

The authors declare no conflict of interests.

### **Funding**

This work was supported by Association against Melanoma Onlus (Italy).

### **Corresponding author:**

Sara Carpi

Department of Pharmacy

University of Pisa

Via Bonanno 6,

56126 PISA

Tel: +39-050-2219539

Fax.: +39-050-2219609

e-mail: sara.carpi@for.unipi.it

## **Abstract**

**Objective.** Human cutaneous melanoma is an aggressive and chemotherapy resistant type of cancer. AM251 is a cannabinoid type 1 (CB1) receptor antagonist/inverse agonist with off-target antitumor activity against pancreatic and colon cancer cells. The current study is aimed at characterizing the *in vitro* anti-melanoma activity of AM251.

**Methods.** The BRAF V600E mutant melanoma cell line, A375, was used as an *in vitro* model system. Characterization tools included cell viability assay, nuclear morphology assessment, gene expression, western blot, flow cytometry with annexin V-FITC/ 7-AAD double staining, cell cycle analyses, measurements of changes in intracellular cAMP and calcium concentrations.

**Results.** AM251 exerted a remarkable cytotoxic effect against A375 human melanoma cells with potency comparable to that observed for cisplatin without significant changes on the human dermal fibroblasts viability. AM251, at a concentration that approximates the IC50, downregulated genes encoding anti-apoptotic proteins (BCL2 and Survivin) and increased transcription levels of pro-apoptotic BAX, induced alteration of annexin V reactivity, DNA fragmentation, chromatin condensation in the cell nuclei, and G2/M phase arrest. AM251 also induced a 40% increase in the basal cAMP levels while it did not affect intracellular calcium concentrations. The involvement of GPR55, TRPA1, and COX-2 in the AM251 mechanism of action was excluded. Combination of AM251 with celecoxib produced a synergistic antitumor activity although the mechanism underlying this effect remains to be elucidated.

**Conclusions.** This study provides the first evidence of a pro-apoptotic effect and G2/M cell cycle arrest of AM251 on A375 cells. This compound may be a potential prototype for the development of promising diarylpyrazole derivatives to be evaluated in human cutaneous melanoma.

**Keywords:** AM251, melanoma, A375 cells, GPR55, TRPA1, cell cycle, apoptosis, Bax, Bcl-2, survivin

## **Introduction**

Cutaneous melanoma, the malignant tumor of melanocytes, is the skin cancer with the greatest mortality and an increasing incidence worldwide [1]. About 50% of melanomas contain a mutation in the proto-oncogene encoding for the serine/threonine kinase B-raf (BRAF) that leads to constitutive activation of downstream signaling in the MAP kinase pathway. In a high percentage of cases, the activating mutation consists of the substitution of valine for glutamate at amino acid 600 (V600E) [2,3], a phenotype correlating with bad prognosis in metastatic melanoma patients [4]. The inhibition of oncogenic B-raf by targeted drugs induces short-lived clinical responses due to the reactivation of signaling downstream of B-raf and the development of acquired resistance in BRAF mutant melanoma patients [5,6]. These notions highlight the need for identification of new prototype compounds aimed at increasing the therapeutic armamentarium for this type of cancer.

Although it is prevalently used as cannabinoid (CB) 1 receptor antagonist/inverse agonist, several lines of evidence demonstrated that the diarylpyrazole derivative AM251 is also characterized by CB-independent biological actions [7-13]. Noteworthy, a remarkable anticancer activity of AM251 has been documented in pancreatic [7,9] and colon cancer cells [9].

The aim of the present study was to characterize the anti-melanoma activity of AM251 against the BRAF V600E mutant cell line, A375, in terms of proapoptotic activity and mechanism of action.

## **Methods**

### *Cell cultures*

The human melanoma A375 cell line (American Type Culture Collection, Rockville, MD, USA) was cultured at 37°C in a humidified atmosphere containing 5% CO<sub>2</sub> in DMEM supplemented with l-glutamine (2 mM), 10% heat-inactivated fetal bovine serum (FBS) and 1% (w/v) penicillin/streptomycin (Sigma-Aldrich, Milan, Italy). Adult human dermal fibroblasts (HDFa; Ref.

C-013-5C, Gibco, Life Technologies, CA, USA) were cultured in an optimized medium containing 5% fetal bovine serum (FBS) and 1% (w/v) penicillin/streptomycin, as recommended by the manufacturer.

### *Drugs*

AM251 (selective CB1 receptor antagonist/inverse agonist and GPR55 agonist), CID16020046 (selective GPR55 antagonist) and forskolin (adenylyl cyclase activator) were obtained from Tocris Bioscience (Northpoint, UK). Cisplatin (CisPt), L- $\alpha$ -lysophosphatidylinositol (LPI), celecoxib, rofecoxib and indomethacin were purchased from Sigma–Aldrich, Milan, Italy. Compounds were dissolved in their specific solvents (DMSO for AM251, CID16020046, LPI and rofecoxib, water for Cis-Pt, and ethanol for others) and further diluted in sterile culture medium immediately before their use. DMSO did never exceed 0.33% v/v in the culture medium.

### *Cell viability assay*

Cell viability was measured using a method based on the cleavage of the 4-(3-(4-iodophenyl)-2-(4-nitrophenyl)-2H-5-tetrazolium)-1,3-benzene disulfonate (WST-1) to formazan by mitochondrial dehydrogenase activity following manufacturer's instructions (Cell proliferation reagent WST-1; Roche, Mannheim, Germany). Briefly, cells ( $5 \times 10^4$ /well) were seeded in 96-well plate in 10% FBS medium; after 24 h, the complete medium was replaced with compound-containing 1% FBS medium. Each compound was dissolved in its specific solvent and then diluted in medium up to the concentrations to be tested. Freshly stock solutions were prepared. AM251 was tested in a concentration range of 0.1–50  $\mu$ M for 24-72 h and its effects evaluated in the presence or absence of different antagonists, selective or non-selective COX-2 inhibitors added 2 h before.

After drug treatment, WST-1 was added and, after 1 h, the absorbance was measured at 450 nm using Infinite® M200 NanoQuant instrument (Tecan, Salzburg, Austria). Optical density values from vehicle-treated cells were considered as 100% cell viability.

### *Transfection*

Cells were transfected with GPR55 siRNA (Santa Cruz Biotechnology, Inc., Santa Cruz, CA, USA, sc-75183) according to the manufacturer's instructions. Briefly, cells were transfected with 100 nM siRNA using Lipofectamine 2000 (Ref. 11668-027, Invitrogen Life Technologies, Carlsbad, CA, USA), which has been reported to yield high transfection efficiency ( $\approx 70\%$ ) in A375 cells [14]. A scrambled non-specific siRNA fluorescent conjugate (Santa Cruz Biotechnology, Inc., Santa Cruz, CA, USA, sc-36869) was used as control and for preliminary confirmation of transfection efficiency through microscope analysis.

### *RT-PCR and quantitative real-time PCR analyses*

Total RNA from cells was extracted by using the RNeasy<sup>®</sup> Mini kit, following manufacturer's instructions, and reverse-transcribed by the QuantiTect<sup>®</sup> Reverse Transcription kit (Qiagen, Valencia, CA, USA). RT-PCRs were performed by the HotStartTaq Master Mix kit (Qiagen, Valencia, CA, USA). Primer sequences are listed in Table 1. Thermal cycle conditions were as follows: 95°C for 15 min, 35 cycles of denaturation at 95°C for 1 min followed by annealing and extension at 72°C for 1 and 10 min, respectively. Detection of the RT-PCR products was performed by agarose gel electrophoresis and ethidium bromide staining.

Real-time PCR was performed with SsoFast Eva Green Supermix (Ref. 172-5201, Bio-Rad, CA, USA). Samples were amplified using the following thermal profile: 95°C for 30 s, 40 cycles of denaturation at 95°C 15 s followed by annealing for 30 s and 72°C for 30 s, with a final step at 65°C for 5 s.  $\beta$ -actin and GAPDH were used as housekeeping genes.

### *Western blot analysis*

Cell lysates were collected after treatment with AM251 at 5  $\mu$ M for 48 h. Samples were transferred and probed with specific antibodies, as previously reported [15]. Quantification of proteins on SDS-

PAGE gels was performed using ImageJ densitometry software and signal intensities were normalized to those for  $\beta$ -actin.

#### *Annexin V and 7-AAD assay*

Dual staining with Annexin V conjugated to fluorescein-isothiocyanate (FITC) and 7-aminoactinomycin (7-AAD) was performed using the commercially available kit (Muse Annexin V and Dead Cell Kit; Merck KGaA, Darmstadt, Germany). Briefly, the treated A375 cells (both floating and adherent cells) were collected and subjected to Annexin V-FITC and 7-AAD staining. Muse<sup>TM</sup> Cell Analyzer measured the sample fluorescence of 10,000 cells. In cells undergoing apoptosis, annexin V bound to phosphatidylserine, which translocated from the inner to the outer leaflet of the cytoplasmic membrane. Double staining was used to distinguish between viable, early apoptotic, or necrotic or late apoptotic cells. Annexin V:FITC positive and 7-AAD negative cells were identified as early apoptotic while Annexin V:FITC positive and 7-AAD positive cells were identified as in late apoptosis or necrosis.

#### *Determination of nuclear morphology*

Changes in nuclear morphology of A375 cells were assessed after treatment with AM251 or its vehicle for 48 h. Cells were fixed with 2% paraformaldehyde on 8-well chamber slides. After washing with PBS, cells were incubated with DAPI 300 nM (Invitrogen Life Technologies, CA, USA ). Fluorescence analysis was realized with Eclipse E600FN Nikon microscope using  $\lambda_{\text{ex}}$  360 nm and  $\lambda_{\text{em}}$  460 nm (magnification  $40 \times$  WD).

#### *cAMP assay*

Intracellular cAMP levels were measured by the cAMP Enzyme Immunoassay Kit (Sigma–Aldrich, Milan, Italy) after treatment with AM251 5  $\mu$ M or forskolin 5  $\mu$ M as positive control. Cell lysates and standards were incubated with a cAMP recognising antibody and incubated at room

temperature in a secondary antibody coated multiwell plate. The excess reagents were then washed away and substrate added. After the incubation time the enzyme reaction was stopped and the yellow color read on a multiwell plate reader at 405 nm (Infinite® M200 NanoQuant; Tecan, Salzburg, Austria).

#### *Fluorescent microscope analysis of $[Ca^{2+}]_i$*

Imaging of  $[Ca^{2+}]_i$  was carried out in A375 cells grown on discs of 35 mm diameter. Fluo-3 AM (Ref. F-1242, Molecular probe, Life Technologies, CA, USA) was added to the culture medium, the cells were incubated for 30 min at 37°C dark and then washed with medium. After 30 min of de-esterification, fluorescence analysis was performed with Eclipse E600FN Nikon microscope (water dipping objective 40X,  $\lambda_{ex}$  490 nm,  $\lambda_{em}$  520 nm) during the perfusion with AM251 and 5  $\mu$ M ionomycin (Calbiochem, Merck Millipore, Darmstadt, Germany) as positive control. The relative fluorescence  $\Delta F/F_0$  was used as an indicator of  $[Ca^{2+}]_i$  in regions of interest.

To determine the  $[Ca^{2+}]_i$  concentrations, Fura-2 AM (Ref. F1201, Molecular probe, Life Technologies, CA, USA) was added to the cells previously treated with AM251 or vehicle for 48 h, for 30 min at 37°C in the dark. After washing with medium and 30 min of de-esterification, fluorescence analysis was performed with Eclipse E600FN Nikon microscope. Loaded cells were alternatively excited at 340 and 380 nm while they were imaged at 510 nm. After background subtraction, ratio images were obtained by dividing, pixel by pixel, pairs of digitized images at 340 and 380 nm. Fluorescence values were converted into ion concentrations, according to Grynkiewicz et al. (1985) [16].

#### *Cell Cycle*

The distribution of cells in the different cycle phases was performed using the Muse™ Cell Analyzer (Merck KGaA, Darmstadt, Germany). Briefly, A375 cells were treated with AM251 (5  $\mu$ M) or its vehicle for 48 and 72 h. Asynchronous adherent cells were collected and centrifuged at

300 × g for 5 minutes. The pellet was washed with PBS and re-suspended in 100 µl of PBS; finally cells were slowly added to 1 ml of ice cold 70% ethanol and maintained o/n at -20°C. Then, a cell suspension aliquot (containing at least 2 × 10<sup>5</sup> cells) was centrifuged at 300 × g for 5 minutes, washed once with PBS and suspended in the fluorescent reagent (Muse™ Cell Cycle reagent). After incubation for 30 minutes at room temperature in the dark, measurements of the percentage of cells in the different phases were acquired.

### *Statistical analysis*

All experiments were performed in triplicate and results were analyzed by GraphPad Prism 5 (GraphPad Software, San Diego, CA, USA). Data were shown as mean values ± standard error of the mean (SEM) obtained from at least three separate experiments. Statistical analyses were performed by Student's *t*-test or one-way ANOVA followed by the Bonferroni's multiple comparison test.

## **Results**

### *Effect of AM251 on cell viability*

AM251 at 0.1-50 µM for 24-72 h induced a concentration- and time-dependent cytotoxicity in A375 cells (Fig. 1A). The IC<sub>50</sub> mean value was 5.52 ± 1.08 µM and 1.79 ± 1.42 µM after 48 and 72 h, respectively, while after 24 h the IC<sub>50</sub> was not reached. The IC<sub>50</sub> of cisplatin (CisPt), the anticancer drug used as reference compound, was 4.33 ± 0.04 µM after 48 h-exposure. Noteworthy, the IC<sub>50</sub> was never reached in human dermal fibroblasts-adult, HDFa treated with AM251 at 0.1-50 µM for 48 and 72 h (Fig.1B).

### *Effect of AM251 on apoptosis*

The role played by the apoptotic process in the AM251-induced cytotoxicity was assessed measuring variation in expression of pro-/anti-apoptotic proteins, morphological changes in the cell



nuclei by fluorescence microscopy, annexin-V and 7-AAD cytofluorometric staining and intracellular calcium concentrations.

AM251 at 5  $\mu$ M for 48 h increased BAX, decreased Survivin and BCL2 gene expression (Fig. 2A), and survivin protein expression (Fig. 2B), as compared to controls. Furthermore, AM251 at 5  $\mu$ M for 72 h markedly increased the number of early and late apoptotic fractions (Fig. 2C) and induced DNA fragmentation and chromatin condensation in the cell nuclei (Fig. 2D), compared to untreated cells.

The role of intracellular calcium in the pro-apoptotic effect induced by AM251 was investigated evaluating the effects of both short and long term treatment of A375 cells. Cells loaded with Fluo-3 did not exhibit detectable changes of fluorescence during treatment with AM251 at concentrations 0.1-10  $\mu$ M, while they responded to ionomycin 5  $\mu$ M, as shown in Fig. 4E. A375 cells loaded with Fura-2 AM and treated with AM251 5  $\mu$ M or vehicle for 48 h did not differ in their intracellular concentration of free calcium, as shown in Fig. 2E.

#### *Effect of AM251 on cell cycle*

The analysis of cell cycle phase distribution of asynchronous cells was assessed by flow cytometry. After treatment with AM251 at 5  $\mu$ M for 48 h the proportion of cells in G0/G1, S and G2/M phases of the cell cycle was 59.2, 14.7 and 20.2%, respectively. The comparison with untreated cells revealed a significant increase of cells in the G2/M and S phases and a decrease of cells in G1/G0 phase (Fig. 3A). Prolonged drug exposure (i.e., 72 h) induced a significant decrease of cells also in the S phase (Fig. 3B), thus confirming the ability of AM251 to promote a cell cycle arrest at G2/M.

#### *Effect of AM251 on intracellular cAMP levels*

A possible influence on cytosolic cAMP content was evaluated in A375 cells exposed to AM251 at 5  $\mu$ M for 48 h. As shown in Fig. 4A, a significant increase (by 40%) in cytosolic cAMP basal levels was observed in treated versus untreated cells.

### *Effect of AM251 on GPR55 and TRPA1*

GPR55 has been recognized as the possible “third” cannabinoid receptor [37,38] with a role in tumorigenesis and metastasis [39-41]. The role of GPR55 on the mechanism of AM251 action was evaluated using gene silencing. 100 nM specific siRNA incubated for 24 and 48 h time-dependently reduced GPR55 mRNA expression by 40.9 and 72.8%, respectively, as compared with scrambled siRNA treated cells (Fig. 4B). No change was induced by siRNA on AM251-induced cytotoxicity (Fig. 4C). Treatment with the potent endogenous GPR55 agonist LPI or the selective GPR55 antagonist, CID16020046, up to 30  $\mu$ M for 48h did not significantly affect cell viability (data not shown).

TRPA1 is expressed in A375 cells [17] and could be a possible target for AM251 [8]. After confirming the presence of TRPA1 by RT-PCR analysis (Fig. 4D), the role of TRPA1 in the AM251-induced cytotoxicity was investigated recording calcium changes immediately after treatment in Fluo 3-AM loaded cells. As shown in Fig. 4E, AM251 at 0.1-10  $\mu$ M did not modify intracellular content of calcium ions, while a clear increase was detectable after the administration of calcium ionophore ionomycin.

### *Role of COX-2 in AM251-induced cytotoxicity*

We previously reported that COX enzymes are expressed in A375 cells [46]. In the current study, we found that treatment of A375 cells with the selective COX-2 inhibitor celecoxib at 0.1-100  $\mu$ M for 48 h induced cytotoxicity with an IC<sub>50</sub> of  $35.64 \pm 1.03$  (Fig. 5A). At variance with this, no effect on cell viability was observed when cells were exposed to rofecoxib (selective COX-2 inhibitor) or indomethacin (non-selective COX inhibitor) (Fig. 5A). Combination of AM251 at 1 and 3  $\mu$ M with selective COX-2 inhibitor, rofecoxib, or non-selective COX-2 inhibitor, indomethacin, did not significantly affect cell viability (data not shown). At variance with this, AM251 *plus* celecoxib produced an anti-proliferative activity greater than that observed for each

drug alone (Fig. 5B). Such an effect appeared to be synergic because it was greater than the sum of the percentage obtained from single treatments.

## **Discussion**

In the current study, we demonstrated that AM251 exerted a remarkable cytotoxic effect against A375 human melanoma cells with potency comparable to that observed for cisplatin. AM251, in the concentration range tested against melanoma cells, did not significantly affect the viability of proliferating human fibroblasts, suggesting that the compound may exhibit some selectivity for cancer cells. To explore in more detail the underlying mechanism of AM251, we assessed whether genes encoding for Bcl-2, Bax and survivin were a target of AM251. Bax and Bcl-2 are two members of the Bcl-2 family that regulates, with opposite effects, the release of cytochrome c in mitochondria-dependent apoptosis [18], whereas survivin is a member of the IAP (inhibiting apoptosis protein) family, which inhibits caspase-9 activation, a typical enzyme involved in the intrinsic apoptotic pathway. In our experimental conditions, the pro-/anti-apoptotic balance drifted to the pro-apoptotic side after treatment of A375 cells with AM251. Specifically, AM251 reduced the expression of anti-apoptotic BCL2 and survivin protein and increased transcription levels of pro-apoptotic BAX. Furthermore, AM251, at a concentration that approximate the IC50 value obtained in cell viability experiments (i.e., 5  $\mu$ M) induced characteristic features of apoptosis, including externalization of phosphatidylserine, DNA fragmentation and chromatin condensation.

Using real-time imaging with the single-wavelength intensity-modulating dye Fluo 3, we did not find changes of intracellular  $\text{Ca}^{2+}$  in A375 cells during treatment with AM251 at 0.1-10  $\mu$ M.

Moreover, dual-wavelength ratiometric indicator Fura-2 allowed us to measure the  $[\text{Ca}^{2+}]_i$  concentrations in cells treated for 48 h with AM251 5  $\mu$ M or vehicle, assessing the maintenance of the intracellular calcium homeostasis in both experimental conditions. These findings suggest that AM251 can induce apoptosis by a specific  $\text{Ca}^{2+}$ -independent mechanism of action. Interesting to note, Gogvadze and co-workers demonstrated a  $\text{Ca}^{2+}$ -independent mechanism of mitochondria

release of cytochrome c via the pro-apoptotic protein Bax [19] and data of the current study showed that AM251 significantly increased BAX expression in A375 cells.

Apoptotic cell death is generally linked to alterations in cell cycle program. The percentage of G0/G1 and S-phase cells was considerably decreased by AM251 and the parallel increase in the proportion of cells in G2/M-phase, in treated *versus* untreated cells, suggests a cell cycle arrest at this level. In line with this, drug-induced arrest in the G2 or M phases may be followed by apoptotic cell death [20] and a pro-apoptotic G2 arrest has been already described in A375 melanoma cells treated with various agents [21-24].

CB1 coupling to the G protein signal transduction pathways transduces the cannabinoid inhibition of adenylyl cyclase, thus attenuating the production of cAMP [25]. It is interesting to note that although the *in vitro* anticancer effect following CB1 receptor activation has been demonstrated in a variety of human cancers [26-30], few data have been provided to substantiate the relationship between such an effect and inhibition of cAMP formation [31]. On the contrary, activation of cyclic nucleotide signaling has been demonstrated to be associated to inhibition of cell proliferation and induction of apoptosis in many cancer cell types [32,33]. For example, elevation of cAMP levels induced by the adenylate cyclase activator, forskolin, or the phosphodiesterase-4 inhibitor, rolipram, induces death of multiple myeloma cells and cAMP-mediated cell death has all the typical hallmarks of apoptosis [34]. In line with its recognized mechanism of action as antagonist/partial inverse agonist at Gi protein-coupled CB1 receptors [35], we observed a 40% increase in the basal cAMP levels on A375 cells treated with a concentration that approximate the IC50 of AM251, suggesting a possible role of cAMP elevation in the *in vitro* anti-melanoma activity of AM251.

AM251 has been recognized to act as agonist/partial agonist at GPR55, the possible “third” cannabinoid receptor [36,37,42,43,44], our findings clearly exclude the involvement of GPR55 in the mechanism of AM251 action. Indeed, the potent endogenous GPR55 agonist, LPI [45] did not affect A375 cell viability and no difference in AM251 activity was observed in GPR55-silenced cells, compared to controls.

AM251 has been also reported to activate the transient receptor potential A1 (TRPA1) in sensory neurons [8] and TRPA1 was found to be expressed in A375 cells [17], a condition that has also been confirmed in the current study. Our findings demonstrated no early rise in  $[Ca^{2+}]_i$  basal levels after treatment of A375 cells with AM251. Since TRPA1 is a non-selective  $Ca^{2+}$  permeable channel, the anticancer effect of AM251 was probably independent of TRPA1 channel activation. Furthermore, data showing that ionic currents through TRPA1 are unlikely responsible for the anti-tumour effects of highly potent TRPA1-activating compounds in A375 cells [17], suggest that this receptor type does not have a major role in determining the phenotype of human melanoma cells.

Taking into account the high levels of cyclooxygenase (COX)-2 expressed in A375 cells [46], we tried to understand whether COX-2 could play a role in AM251 cytotoxicity. While celecoxib induced cytotoxicity in A375 cells, with a potency lower than that observed for AM251, other selective (rofecoxib) and non-selective (indomethacin) COX-2 inhibitors did not. Combination of AM251 with rofecoxib or indomethacin did not significantly affect cell viability, whereas AM251 *plus* celecoxib displayed synergistic antiproliferative activity in A375 cells. While these findings reinforce the concept that COX-2 inhibition did not play a role in AM251 cytotoxicity, they highlight need for further investigation on the mechanistic bases of AM251-celecoxib combination in human cutaneous melanoma.

It is interesting to note that COX-2-inhibitory function is not required for celecoxib-mediated apoptosis, which seems to be associated to the unbalance between pro- e anti-apoptotic proteins, the activation of intrinsic apoptotic pathway, and the delayed progression of cells through the G2/M phase of the cell cycle [47-48]. Our findings are in line with the previously reported celecoxib-AM251 molecular similarity [7], which may represent the basis for further investigation on the molecular mechanism of AM251. Overall, the results of the current study suggest that AM251 could be a prototypical compound for the development of promising diarylpyrazole derivatives in human cutaneous melanoma.

## References

- 1 Jemal A, Siegel R, Xu J, Ward E. Cancer statistics, 2010. *CA Cancer J Clin* 2010;60: 277-300.
- 2 Finn L, Markovic S, Joseph R. Therapy for metastatic melanoma: the past, present, and future. *BMC Med*. 2012;10:23.
- 3 Holderfield M, Deuker M, McCormick F, McMahon M. Targeting RAF kinases for cancer therapy: BRAF-mutated melanoma and beyond. *Nat Rev Cancer* 2014;14:455-467.
- 4 Picard M, Pham Dang N, D'Incan M, Mansard S, Dechelotte P, Pereira B et al. Is BRAF a prognostic factor in stage III skin melanoma? A retrospective study of 72 patients after positive sentinel lymph node dissection. *Br J Dermatol*. 2014;171:108-114.
- 5 Hu-Lieskovan S, Robert L, Homet Moreno B, Ribas A. Combining targeted therapy with immunotherapy in BRAF-mutant melanoma: promise and challenges. *J Clin Oncol*. 2014;32: 2248-2255.
- 6 Karimkhani C, Gonzalez R, Dellavalle R. A review of novel therapies for melanoma. *Am J Clin Dermatol*. 2014;15:323-337.
- 7 Fogli S, Nieri P, Chicca A, Adinolfi B, Mariotti V, Iacopetti P et al. (2006). Cannabinoid derivatives induce cell death in pancreatic MIA PaCa-2 cells via a receptor-independent mechanism. *FEBS Lett*. 2006;580:1733-1739.
- 8 Patil M, Patwardhan A, Slas M, Hargreaves K, Akopian A. Cannabinoid receptor antagonists AM251 and AM630 activate TRPA1 in sensory neurons. *Neuropharmacology* 2011;61:778-788.
- 9 Fiori JL, Sanghvi M, O'Connell MP, Krzysik-Walker SM, Moaddel R, Bernier M. The cannabinoid receptor inverse agonist AM251 regulates the expression of the EGF receptor and its ligands via destabilization of oestrogen-related receptor  $\alpha$  protein. *Br J Pharmacol* 2011;164: 1026-1040.
- 10 Raffa R, Ward S . CB<sub>1</sub>-independent mechanisms of  $\Delta^9$ -THCV, AM251 and SR141716 (rimonabant). *J Clin Pharm Ther*. 2012;37:260-265 .

- 11 Seely K, Brents LK, Franks LN, Rajasekaran M, Zimmerman SM, Fantegrossi WE, et al. AM-251 and rimonabant act as direct antagonists at mu-opioid receptors: implications for opioid/cannabinoid interaction studies. *Neuropharmacology* 2012;63:905-915.
- 12 Baur R, Gertsch J, Sigle E. The cannabinoid CB1 receptor antagonists rimonabant (SR141716) and AM251 directly potentiate GABA(A) receptors. *Br J Pharmacol* 2012;165: 2479-2484.
- 13 Krzysik-Walker S, González-Mariscal I, Scheibye-Knudsen M, Indig F, Bernier M. The biarylpyrazole compound AM251 alters mitochondrial physiology via proteolytic degradation of  $ERR\alpha$ . *Mol Pharmacol* 2013;83:157-166.
- 14 Zhou L, Chen Z, Wang F, Yang X, Zhang B. Multifunctional triblock co-polymer mP3/4HB-b-PEG-b-IPEI for efficient intracellular siRNA delivery and gene silencing. *Acta Biomater* 2013;9:6019-6031.
- 15 Carpi S, Fogli S, Giannetti A, Adinolfi B, Tombelli S, Da Pozzo E, et al. Theranostic properties of survivin-directed molecular beacon in human melanoma cells. *Plos One* 2014;9:e114588.
- 16 Grynkiewicz G, Poenie M, Tsien RY (1985). A new generation of  $Ca^{2+}$  indicators with greatly improved fluorescence properties. *J Biol Chem*. 1985; 260:3440–3450.
- 17 Oehler B, Scholze A, Schaefer M, Hill K (2012). TRPA1 is functionally expressed in melanoma cells but is not critical for impaired proliferation caused by allyl isothiocyanate or cinnamaldehyde. *Naunyn Schmiedebergs Arch Pharmacol*. 2012;385:555-563.
- 18 Elmore S Apoptosis: a review of programmed cell death. *Toxicol Pathol* 2007;35: 495-516.
- 19 Gogvadze V, Robertson JD, Zhivotovsky B, Orrenius S . Cytochrome c release occurs via  $Ca^{2+}$ -dependent and  $Ca^{2+}$ -independent mechanisms that are regulated by Bax. *J Biol Chem* 2001;276: 19066-19071.
- 20 DiPaola RS. To arrest or not to G(2)-M Cell-cycle arrest : commentary re: A. K. Tyagi et al., Silibinin strongly synergizes human prostate carcinoma DU145 cells to doxorubicin-induced growth inhibition, G(2)-M arrest, and apoptosis. *Clin cancer res* 2002;8: 3311-3314.

- 21 Wei G, Wang S, Cui S, Guo J, Liu Y, Liu Y, et al. Synthesis and evaluation of the anticancer activity of albiziabioside A and its analogues as apoptosis inducers against human melanoma cells. *Org Biomol Chem* 2014;12: 5928-5935.
- 22 Huang H, Wang X, Ding X, Xu Q, Hwang SK, Wang F et al. . Effect and mechanism of tacrolimus on melanogenesis on A375 human melanoma cells. *Chin Med J (Engl)* 2014;127: 2966-2971.
- 23 Das S, Das J, Samadder A, Boujedaini N, Khuda-Bukhsh AR. Apigenin-induced apoptosis in A375 and A549 cells through selective action and dysfunction of mitochondria. *Exp Biol Med* 2012;237:1433-1448.
- 24 Huang SH, Wu LW, Huang AC, Yu CC, Lien JC, Huang YP et al.. Benzyl isothiocyanate (BITC) induces G2/M phase arrest and apoptosis in human melanoma A375.S2 cells through reactive oxygen species (ROS) and both mitochondria-dependent and death receptor-mediated multiple signaling pathways. *J Agric Food Chem* 2012;60:665-675.
- 25 Pertwee R. Receptors and channels targeted by synthetic cannabinoid receptor agonists and antagonists. *Curr Med Chem* 2010;17:1360-1381.
- 26 De Petrocellis L, Melck D, Palmisano A, Bisogno T, Laezza C, Bifulco M, et al. The endogenous cannabinoid anandamide inhibits human breast cancer cell proliferation. *Proc Natl Acad Sci U S A* 1998;95: 8375-8380.
- 27 Bifulco M, Laezza C, Portella G, Vitale M, Orlando P, De Petrocellis L, et al.. Control by the endogenous cannabinoid system of ras oncogene-dependent tumor growth. *FASEB J.* 2001;15: 2745-2747.
- 28 Portella G, Laezza C, Laccetti P, De Petrocellis L, Di Marzo V, Bifulco M . Inhibitory effects of cannabinoid CB1 receptor stimulation on tumor growth and metastatic spreading: actions on signals involved in angiogenesis and metastasis. *FASEB J* 2003;17:1771-1773.



- 29 Blázquez C, Carracedo A, Barrado L, Real PJ, Fernández-Luna JL, Velasco G, et al.. Cannabinoid receptors as novel targets for the treatment of melanoma. *FASEB J.* 2006;20: 2633-2635.
- 30 Kenessey I, Bánki B, Márk A, Varga N, Tóvári J, Ladányi A, et al.. Revisiting CB1 receptor as drug target in human melanoma. *Pathol Oncol Res* 2012;18: 857-866.
- 31 Melck D, Rueda D, Galve-Roperh I, De Petrocellis L, Guzmán M, Di Marzo V. Involvement of the cAMP/protein kinase A pathway and of mitogen-activated protein kinase in the anti-proliferative effects of anandamide in human breast cancer cells. *FEBS Lett* 1999;463: 235-240.
- 32 Lucchi S, Calebiro D, de Filippis T, Grassi ES, Borghi MO, Persani L . 8-Chloro-cyclic AMP and protein kinase A I-selective cyclic AMP analogs inhibit cancer cell growth through different mechanisms. *PLoS One* 2011;6:e20785.
- 33 Fajardo AM, Piazza GA, Tinsley HN. The role of cyclic nucleotide signaling pathways in cancer: targets for prevention and treatment. *Cancers (Basel)* 2014;6:436-458.
- 34 Follin-Arbelet V, Hofgaard PO, Hauglin H, Naderi S, Sundan A, Blomhoff R et al. Cyclic AMP induces apoptosis in multiple myeloma cells and inhibits tumor development in a mouse myeloma model. *BMC Cancer* 2011;11:301.
- 35 Fišar Z, Singh N, Hroudová J Cannabinoid-induced changes in respiration of brain mitochondria. *Toxicol Lett* 2014;231:62-71.
- 36 Brown A . Novel cannabinoid receptors. *Br J Pharmacol.* 2007;152: 567-575.
- 37 Ryberg E, Larsson N, Sjögren S, Hjorth S, Hermansson NO, Leonova J, et al. The orphan receptor GPR55 is a novel cannabinoid receptor. *Br J Pharmacol* 2007;152: 1092-1101.
- 38 Moriconi A, Cerbara I, Maccarrone M, Topai A. GPR55: Current knowledge and future perspectives of a purported "Type-3" cannabinoid receptor. *Curr Med Chem* 2010;17: 1411-1429.
- 39 Piñeiro R, Maffucci T, Falasca M . The putative cannabinoid receptor GPR55 defines a novel autocrine loop in cancer cell proliferation. *Oncogene* 2011;30:142-152.

- 40 Andradas C, Caffarel MM, Pérez-Gómez E, Salazar M, Lorente M, Velasco G, et al. The orphan G protein-coupled receptor GPR55 promotes cancer cell proliferation via ERK. *Oncogene* 2011;30: 245-252.
- 41 Paul RK, Wnorowski A, Gonzalez-Mariscal I, Nayak SK, Pajak K, Moaddel R et al. (R,R')-4'-methoxy-1-naphthylfenoterol targets GPR55-mediated ligand internalization and impairs cancer cell motility. *Biochem Pharmacol* 2014;87: 547-556.
- 42 Kapur A, Zhao P, Sharir H, Bai Y, Caron M, Barak L, et al.. Atypical responsiveness of the orphan receptor GPR55 to cannabinoid ligands. *J Biol Chem* 2009;284: 29817-29827.
- 43 Sharir H, Abood M. Pharmacological characterization of GPR55, a putative cannabinoid receptor. *Pharmacol Ther.* 2010;126: 301-313.
- 44 Anavi-Goffer S, Baillie G, Irving AJ, Gertsch J, Greig IR, Pertwee RG, et al. . Modulation of L- $\alpha$ -lysophosphatidylinositol/GPR55 mitogen-activated protein kinase (MAPK) signaling by cannabinoids. *J Biol Chem.* 2012;287: 91-104.
- 45 Yamashita A, Oka S, Tanikawa T, Hayashi Y, Nemoto-Sasaki Y, Sugiura T. The actions and metabolism of lysophosphatidylinositol, an endogenous agonist for GPR55. *Prostaglandins Other Lipid Mediat.* 2013;107: 103-116.
- 46 Adinolfi B, Romanini A, Vanni A, Martinotti E, Chicca A, Fogli S, et al. (2013). Anticancer activity of anandamide in human cutaneous melanoma cells. *Eur J Pharmacol.* 2013;718: 154-159.
- 47 Grösch S, Maier TJ, Schiffmann S, Geisslinger G. Cyclooxygenase-2 (COX-2)-independent anticarcinogenic effects of selective COX-2 inhibitors. *J Natl Cancer Inst.* 2006;98: 736-747.
- 48 Păunescu H, Coman OA, Coman L, Ghiță I, Georgescu SR, Drăghia F et al. Cannabinoid system and cyclooxygenases inhibitors. *J Med Life.* 2011;4:11-20.

## Tables

**Table 1.** Primer nucleotide sequences, Ta and amplicon length used for PCR experiments.

| Protein        | Primer nucleotide sequences  | Ta (°C) | Amplicon length |
|----------------|--|---------|-----------------|
| $\beta$ -actin | 5'-AACTGGAACGGTGAAGGTGAC-3' (F)<br>5'-GACTTCCTGTAACAACGCATCTC-3' (R) | 61      | 138 pb          |
| GAPDH          | 5'-GTGAAGGTCGGAGTCAACG-3' (F)<br>5'-GGTGAAGACGGCCAGTGGACT-3' (R)     | 59      | 301 pb          |
| TRPA1          | 5'-TCACCATGAGCTAGCAGACTATTT-3' (F)<br>5'-GAGAGCGTCCTTCAGAATCG-3' (R) | 55      | 74 pb           |
| Bax            | 5'-TCTGACGGCAACTTCAACTG-3' (F)<br>5'-TTGAGGAGTCTCACCCAACC-3' (R)     | 56,6    | 188 pb          |
| Bcl-2          | 5'-TCCATGTCTTTGGACAACCA-3' (F)<br>5'-CTCCACCAGTGTTCCCATCT-3' (R)     | 56,6    | 203 pb          |
| Survivin       | 5'-ACCAGGTGAGAAGTGAGGGA-3' (F)<br>5'-AACAGTAGAGGAGCCAGGGA-3' (R)     | 59      | 309 pb          |

## Figure legends

**Figure 1.** Time-dependency and selectivity of AM251 activity: A) Concentration-dependent cell viability decrease to AM251, in A375 melanoma cells after 24, 48 and 72 h exposure to a single drug administration; B) Concentration-response curves to AM251 in HDFa cells after 48 and 72h exposure. Data are the mean  $\pm$  SEM from three independent experiments. \*\*P<0.01; \*\*\*P<0.001, as compared with 24 h (ANOVA followed by the Bonferroni's multiple comparison test).

**Figure 2.** Apoptosis induced by AM251 in A375 cells: A) Real-time PCR for the three protein involved in apoptosis in A375 treated with AM251 for 48 h. Values were expressed as mean  $\pm$  standard of the mean (SEM) from three separate experiments. \*\*\*P<0.001 (ANOVA followed by the Bonferroni's multiple comparison test). B) Western Blot analysis of survivin protein levels followed by densitometric assay in A375 cells treated with AM251 for 48 h. C) Analysis of annexin V- 7AAD double staining in A375 cells after treatment with AM251 at 5  $\mu$ M for 72 h or vehicle. Upper: Representative dot plots. Lower: bar graph. \*\*P<0.01; \*\*\*P<0.001 (ANOVA followed by the Bonferroni's multiple comparison test). D) Nuclear morphology revealed by DAPI staining of A375 cells treated with AM251 or vehicle at 48 h. E)  $[Ca^{2+}]_i$  levels in Fura-2 AM loaded A375 cells after treatment for 48 h with AM251 or vehicle (CNTR). Mean values  $\pm$  SEM (n = 160, P = 0.35 Student t test).

**Figure 3.** Cell cycle analyses for asynchronized A375 cells treated with AM251 or vehicle. Percentage of A375 cell cycle phases after AM251 at 5  $\mu$ M for A) 48 and B) 72 h. Data are presented as percentage change of cells in the different phases (G0/G1, G2 or S) versus control cells and represent the mean  $\pm$  SEM of three different experiments.

**Figure 4.** A) cAMP increase in A375 cells after AM251 (5 $\mu$ M) treatment at 48h. Data are the mean  $\pm$  SEM from three experiments. \*\*\* P<0.001 from Student's *t*-test. B) Real-time PCR results for GPR55 expression, referred to the housekeeping gene beta-actin, after 24 h and 48h after siRNA treatment compared to control siRNA-treated cells. \*\*\* P<0.001 from ANOVA and Bonferroni test C) Concentration-response curve to AM251 in non-treated cells and in cells silenced with GPR55 siRNA. D) Ethidium-bromide stained agarose gel revealing TRPA1 gene expression (74pb band) in A375 cells E) Absence of changes in Fluo-3 fluorescence during treatment with AM251 (0.1-10  $\mu$ M) and increase of signal after calcium loading induced by ionomycin 5  $\mu$ M. The black and red traces indicate the mean pixel values in the regions of interest marked by circles. On the pseudocolor scale blue represents 0 and red 255.

**Figure 5.** (A) Concentration-response curves to celecoxib, rofecoxib and indomethacin in A375 cells after 48 h exposure. Data are the mean  $\pm$  SEM from three independent experiments. (B) Cell viability after combination of AM251 at 1 and (C) 3  $\mu$ M with selective (rofecoxib and celecoxib) or non-selective (indomethacin) COX inhibitors, compared to single treatments. Values were expressed as mean  $\pm$  standard of the mean (SEM) from three separate experiments. \*\*\*P<0.001, compared with AM251 alone; ###P<0.001, compared with celecoxib alone (ANOVA followed by the Bonferroni's multiple comparison test).

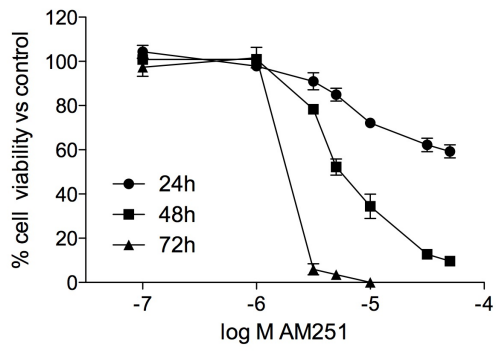
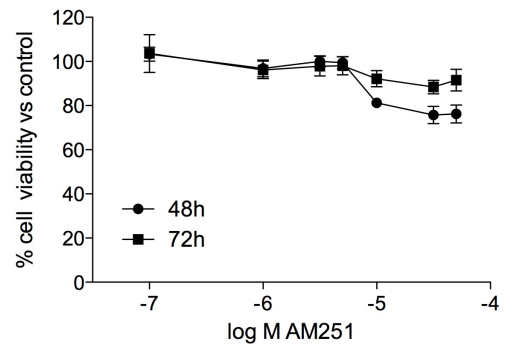
**A****B**

Figure 1

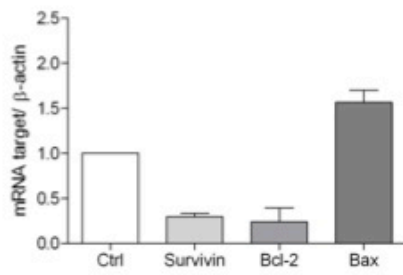
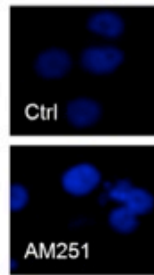
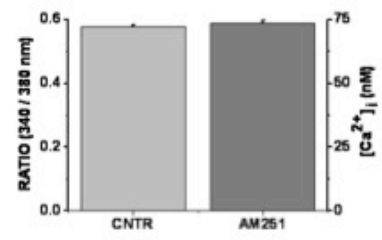
**A****B****C**

Figure 2

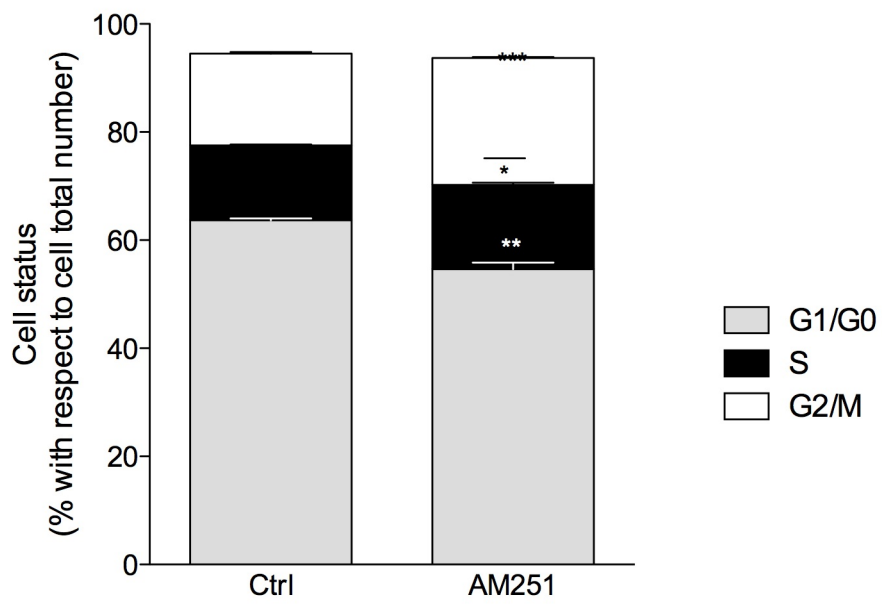
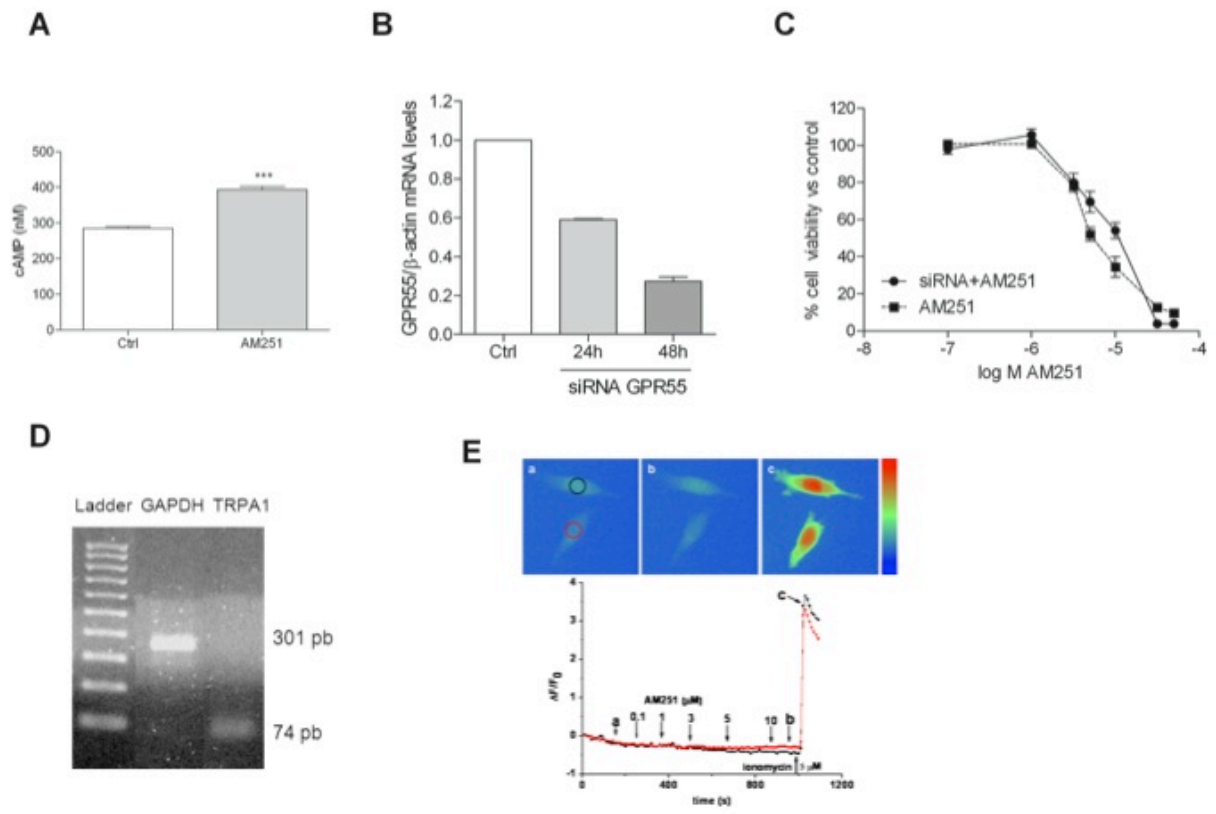


Figure 3





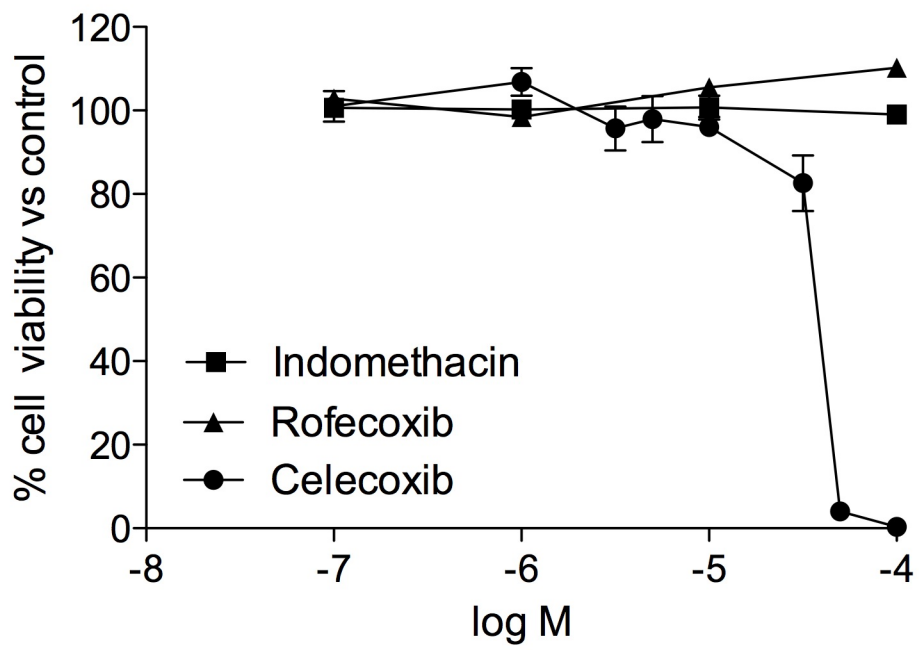


Figure 5